Virology 531 (2019) 183–191

Contents lists available at ScienceDirect

Virology

journal homepage: www.elsevier.com/locate/virology

Human metapneumovirus infection of airway epithelial cells is associated with changes in core metabolic pathways

Yanhua Zhao[a], Harendra Singh Chahar[a], Narayana Komaravelli[a], Anar Dossumekova[a], Antonella Casola[a,b,c,d,*]

[a] Dept. of Pediatrics, University of Texas Medical Branch, Galveston, TX, USA
[b] Dept. of Microbiology, University of Texas Medical Branch, Galveston, TX, USA
[c] Sealy Center for Vaccine Development, University of Texas Medical Branch, Galveston, TX, USA
[d] Sealy Center for Molecular Medicine, University of Texas Medical Branch, Galveston, TX, USA

ARTICLE INFO

Keywords:
Human metapneumovirus
Metabolism
Glycolysis
TCA cycle
Virus replication

ABSTRACT

Human metapneumovirus (hMPV) is an important cause of acute lower respiratory tract infections in infants, elderly and immunocompromised individuals. Ingenuity pathway analysis of microarrays data showed that 20% of genes affected by hMPV infection of airway epithelial cells (AECs) were related to metabolism. We found that levels of the glycolytic pathway enzymes hexokinase 2, pyruvate kinase M2, and lactate dehydrogenase A were significantly upregulated in normal human AECs upon hMPV infection, as well as levels of enzymes belonging to the hexosamine biosynthetic and glycosylation pathways. On the other hand, expression of the majority of the enzymes belonging to the tricarboxylic acid cycle was significantly diminished. Inhibition of hexokinase 2 and of the glycosylating enzyme O-linked N-acetylglucosamine transferase led to a significant reduction in hMPV titer, indicating that metabolic changes induced by hMPV infection play a major role during the virus life cycle, and could be explored as potential antiviral targets.

1. Introduction

Viruses are obligate parasites and completely depend on host cells for resources necessary for virus growth and reproduction. Lack of their own metabolic system forces viral pathogens to exploit host cells to synthesize viral proteins and genome, whether it is DNA or RNA. Nucleic acid and protein synthesis requires not only significant amount of energy but also the raw materials for biomolecule synthesis and enhanced glucose and glutamine utilizations provide the required energy and building blocks in virus infected cells (Chambers et al., 2010; Munger et al., 2006, 2008). Such dependence on host warrants that viruses should have mechanisms in place that allow viruses to manipulate host cell metabolism to facilitate their growth and replication. Indeed, mounting evidence suggest that a variety of evolutionarily divergent viruses modify metabolic activities of the host cells upon infection, inhibit cellular processes such as proliferation and cellular macromolecular synthesis in order to re-route the valuable resources to their own replication (Sanchez and Lagunoff, 2015).

Human metapneumovirus (hMPV) is a non-segmented negative sense RNA virus belonging to the *Pneumoviridae* family, according to the new taxonomy of the order *Mononegavirales* (Afonso et al., 2016). HMPV causes upper and lower respiratory tract infections in people of all ages, but can cause serious illness in children younger than 1 year of age, the elderly and immunocompromised individuals. Usually the symptoms include cough, runny nose, nasal congestion, sore throat, and fever, but in high risk groups, symptoms may include wheezing, dyspnea, hoarseness, pneumonia, and a flare-up of asthma (Kahn, 2006). There is still no effective treatment or vaccine for this virus infection in part due to the poor understanding of many fundamental questions regarding the pathogenesis of hMPV-induced lung disease.

Under normal conditions, the respiratory epithelium represents the principal cellular barrier between the environment and the internal milieu of the airways and is responsible for particulate clearance and surfactant secretion. The airway epithelial cells are the primary target of hMPV infection (Biacchesi et al., 2006). In a previous study, we used high density oligonucleotide probe-based cDNA microarrays to investigate host transcriptional responses induced by hMPV infection of airway epithelial cells. Our results demonstrated that hMPV induced significant changes in epithelial cell global gene expression in a time-dependent fashion, in particular changes in signaling pathway leading to the induction of inflammatory and immunomodulatory molecules, as well as a variety of metabolic pathways (Bao et al., 2008). Like other

* Correspondence to: Department of Pediatrics, University of Texas Medical Branch, 301 University Blvd, Galveston, TX 77555, USA.
E-mail address: ancasola@utmb.edu (A. Casola).

https://doi.org/10.1016/j.virol.2019.03.011
Received 22 October 2018; Received in revised form 15 March 2019; Accepted 19 March 2019
Available online 22 March 2019
0042-6822/

viruses, hMPV is also dependent upon host cells for energy and molecular subunits to assemble viral progeny, however, little or nothing is known about what kind of metabolic changes hMPV induces in airway epithelial cells upon infection.

In the present study, analysis of microarray data identified specific genes of cellular metabolic pathways, namely glycolysis (GLY), hexosamine biosynthesis pathway (HBP), pentose phosphate pathway (PPP) and tricarboxylic acid cycle (TCA), modulated by hMPV upon infection. LCMS/GCMS-based metabolomics analysis confirmed virus-induced changes in cellular levels of key metabolites of the GLY/PPP/TCA pathways. Inhibition of glycolysis and HBP/glycosylation pathway led to a significant reduction of hMPV viral titers, indicating that they play an essential for efficient virus replication. These findings provide improved understanding of viral manipulation of host cell metabolism and may lead to the discovery of newer antiviral therapeutic approaches based on metabolic pathway inhibitors.

2. Results

2.1. HMPV infection alters metabolic pathways in airway epithelial cells

In one of our previous studies, we utilized high-density microarrays analysis using Bonferroni test to investigate changes in gene expression induced by hMPV infection in A549 cells, a cancer cell line retaining features of type II alveolar epithelial cells (Bao et al., 2008). Further statistical analysis, using Benjamin Hochs for a more discovery-type approach, revealed that expression of 9750 genes was significantly modified over a period of 72 h in infected cells, compared to mock-infected, indicating that hMPV induces profound changes in global gene transcription. The list of all targets affected by hMPV infection is summarized in Supplementary Table 1 (ST1). Of these transcripts, 8907 genes were mapped to IPA (Ingenuity Pathway Analysis) database, and 5164 genes were categorized by Biological and Function analysis. The biological category distribution of the genes affected by hMPV infection is summarized in Fig. 1. Of the 5164 differentially expressed genes, a significant portion, approximately 20%, was associated with cellular metabolic pathways. The list of all canonical pathways affected by hMPV infection is summarized in Supplementary Table 2 (ST2).

We further categorized the genes related to cellular metabolism into major central metabolic pathways using IPA analysis. We found that 257 genes belonged to lipid, fatty acid and steroid metabolism; 197 genes to amino acid, peptide and protein metabolism; 180 genes belonged to mineral, vitamin, hormones, coenzyme and co-factor metabolism; 148 genes belonged to carbohydrate metabolism and 90 genes were involved in nucleoside, nucleotide and nucleic acid metabolism (Fig. 2). The large number of genes modulated in various metabolic pathways suggests how effectively hMPV infection can trigger changes in infected cells and these data clearly demonstrate that most of the metabolic pathways in the airway epithelial cells are manipulated by hMPV infection.

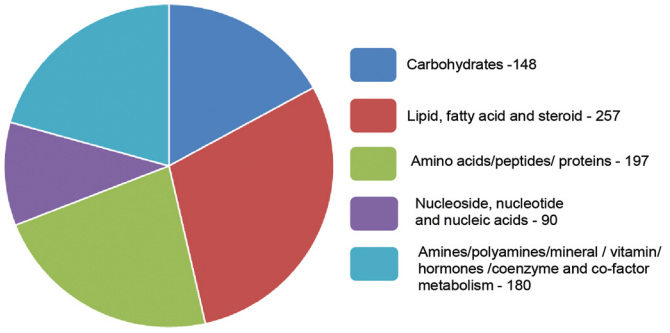

Fig. 2. Number of genes in the microarray database differentially expressed upon hMPV infection belonging to IPA canonical metabolic pathways.

2.2. HMPV infection induces changes of key enzymes of the glycolytic pathway

Our metabolic pathway analysis identified significant changes in the expression of genes belonging to the central carbohydrate and energy metabolic pathways upon hMPV infection, in particular the glycolysis, TCA and PPP pathways (Table 1). Glucose serves as the primary fuel source for mammalian cells and is metabolized to generate pyruvate through the glycolysis pathway. Under normal circumstances, most of the pyruvate enters the mitochondria and is oxidized by the TCA/Krebs Cycle to generate ATP. However, in certain metabolic conditions including oncogenic transformation and some infections, a significant amount of the pyruvate generated in glycolysis is diverted to lactate dehydrogenase (LDH)-mediated lactic acid production by switching expression of the rate-limiting enzyme PKM1 to the PKM2 isoform. This re-routing of pyruvate to lactate production is called “Warburg effect”, as well as aerobic glycolysis since it occurs in presence of oxygen (Vander et al., 2009). To confirm the changes we observed in expression of genes belonging to the central carbohydrate and energy metabolic pathways in A549 cells, a lung carcinoma-derived cell line, we investigated expression levels of the key rate-limiting enzymes of the glycolytic pathway HK2 and PMK2 in human small airway epithelial (SAE) cells isolated from normal human lung tissue. We found that HK2 protein levels were significantly increased at 15 and 24 p.i by several fold (Fig. 3). Similarly, PMK2 expression was significantly upregulated in response to hMPV infection in a time-dependent manner (Fig. 3). These observations strongly suggested that hMPV induces a metabolic shift driving the cellular metabolism towards aerobic glycolysis by manipulating key enzymes of the glycolysis pathway.

Lactate dehydrogenase A (LDHA) is present in most somatic tissues, predominantly in muscle tissue and tumors, and catalyzes the conversion of pyruvate into lactate. In the presence of oxygen, this pyruvate generated from glucose supplies energy by entering the TCA cycle (aerobic respiration), however, lack of oxygen pushes the pyruvate to glycolytic pathway to produce lactate. To determine expression levels of LDHA, total cell lysate of SAE cells infected with hMPV and harvested

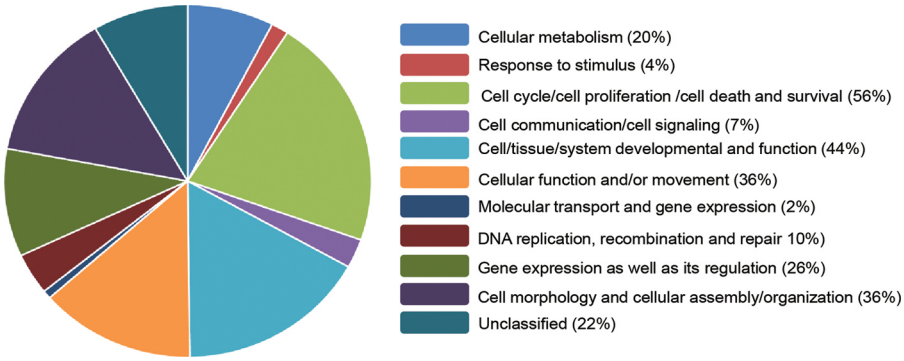

Fig. 1. The biological category distribution of the genes (%) affected by hMPV infection. Differently expressed genes mapped in IPA (Ingenuity Pathway Analysis) database were clustered for the Biological and Function by IPA analysis. Total input genes at p-value 0.01 after BH analysis = 9750; IPA Mapped: 8907, IPA Unmapped: 843; IPA Analysis Ready: 6226 of which 5164 were used for Biological and Function analysis.

Table 1
Gene expression changes in the central carbohydrate and energy metabolic pathways upon hMPV infection.

Pathway	Gene	Entrez Gene Name	Fold change	
			24 h	48 h
Glycolysis	HK2	hexokinase 2	2.2	3.3
	PGI	glucose-6-phosphate isomerase	-1.2	-3.2
	PFK	phosphofructokinase, muscle	-1.1	-1.9
	TPI	triosephosphate isomerase 1	-1.4	-2.2
	GAPDH	glyceraldehyde-3-phosphate dehydrogenase	-1.1	-1.6
	PGK	phosphoglycerate kinase 1	-1.0	-2.0
	ENO2	enolase 2	-1.0	-1.4
TCA	MDH1	malate dehydrogenase 1	-1.4	-3.7
	SDHA	succinate dehydrogenase complex, subunit A	-1.2	-2.0
	SDHC	succinate dehydrogenase complex, subunit C	-1.3	-2.3
	IDH3A	isocitrate dehydrogenase 3 (NAD+) alpha	-1.3	-2.0
	SDHB	succinate dehydrogenase complex, subunit B	-1.0	-1.9
	FH	fumarate hydratase	-1.4	-3.2
	ACO1	aconitase 1, soluble	-2.0	-1.9
	CS	citrate synthase	-1.2	-2.0
	MDH2	malate dehydrogenase 2, NAD	-1.4	-1.7
	SUCLG1	succinate-CoA ligase, alpha subunit	-1.4	-2.3
	DHTKD1	dehydrogenase E1 and transketolase domain containing 1	1.1	-1.2
Oxidative phosphorylation	**Complex I:**			
	NDUFA1	NADH dehydrogenase (ubiquinone) 1 alpha subcomplex, 1	-1.2	-2.4
	NDUFB1	NADH dehydrogenase (ubiquinone) 1 beta subcomplex, 1	-1.3	-2.5
	NDUFS8	NADH dehydrogenase (ubiquinone) Fe-S protein 8	-1.3	-3.5
	Complex II:	succinate dehydrogenase complex, subunit A	-1.2	-2.0
	SDHA	succinate dehydrogenase complex, subunit B	-1.0	-1.9
	SDHB	succinate dehydrogenase complex, subunit C	-1.3	-2.3
	SDHC	ubiquinol-cytochrome c reductase binding protein	-1.3	-2.3
	Complex III:	ubiquinol-cytochrome c reductase, complex III subunit VII	-1.2	-2.7
	UQCRB	ubiquinol-cytochrome c reductase core protein II	-1.2	-2.2
	UQCRQ	cytochrome c oxidase subunit Va	-1.4	-1.7
	UQCRC2	cytochrome c oxidase subunit VIIb	-1.4	-1.9
	Complex IV:	cytochrome c oxidase subunit VIb polypeptide 1	-1.3	-2.2
	COX5A	ATP synthase, H+ transporting, O subunit	-1.1	-2.5
	COX7B	ATP synthase, H+ transporting, beta polypeptide	-1.3	-2.6
	COX6B1	ATP synthase, H+ transporting, epsilon subunit	-1.0	-1.7
	ATP synthase:			
	ATP5O			
	ATP5B			
	ATP5E			
Pentose phosphate pathway	PGD	phosphogluconate dehydrogenase	-1.2	-2.9
	TALDO1	transaldolase 1	-1.2	-2.7
	G6PD	glucose-6-phosphate dehydrogenase	-1.1	-4.0
	TKT	transketolase	-1.3	−3.0
	RPIA	ribose 5-phosphate isomerase A	-1.1	-1.7
	H6PD	hexose-6-phosphate dehydrogenase (glucose 1-dehydrogenase)	1.1	1.4
Glycosylation pathway/ hexosamine biosynthetic pathway	OGT	O-linked N-acetylglucosamine (GlcNAc) transferase	1.1	1.8
	GFPT1	glutamine–fructose-6-phosphate transaminase 1	2.1	2.4
	GFPT2	glutamine-fructose-6-phosphate transaminase 2	1.7	3.1
	PGM3	phosphoglucomutase 3	1.6	1.8
	MGEA5	meningioma expressed antigen 5 (hyaluronidase)	1.2	1.4

at various time points p.i. were analyzed by Western blot. We found that LDHA protein level started to increase at 6 h p.i. and remain elevated till 24 h p.i. (Fig. 3).

2.3. hMPV infection induces a core metabolic shift in human primary airway epithelial cells

To confirm changes in the core metabolic pathways, SAE cells were infected with hMPV and whole cell lysate was subjected to gas chromatography-mass spectrometry (GC/MS) and liquid chromatography-mass spectrometry (LC/MS)-based glycolysis/TCA/PPP metabolomics analysis. For the glycolysis pathway, we found that hMPV infection led to an initial increase (at 6 h p.i.) of most of the metabolites belonging to the pathway, however, there was a subsequent decrease of all of them, as infection progressed, with the exception of fructose 6-Phosphate/ glucose-6-phosphate and lactic acid levels, which were higher than basal levels throughout the duration of infection (Fig. 4**A**). Levels of most of the metabolites belonging to the TCA and PPP pathways also progressively decreased at later time points of infection (15 and 24 h p.i.), with the exception of Acetyl-CoA, citrate and ADP (Fig. 4**B** and **C**).

2.4. hMPV infection upregulated key enzymes in hexosamine biosynthesis pathway

Typically glucose transported inside the cell is phosphorylated into glucose-6-phosphateand enters the glycolysis pathway to provide energy. However, part of glucose is directed into the hexosamine biosynthetic pathway (HBP) to promote protein glycosylation. Most proteins that are secreted, or membrane-bounded, are covalently attached by carbohydrate to form glycoproteins, through either O-glycosidic or N-glycosidic bonds. These glycoproteins are involved in the metabolism of amino acids, nucleotides and carbohydrates, general metabolic pathways, cell growth and maintenance, DNA damage responses, intracellular transport, transcription. Glycoprotein synthesis is necessary for enveloped virus replication as they are usually responsible for the attachment and entry of host cells, leading to productive infection

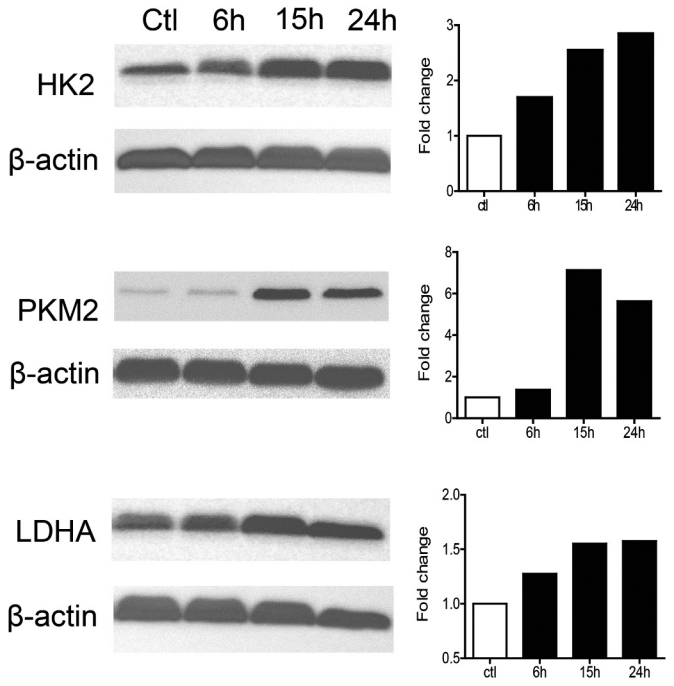

Fig. 3. Cellular levels of HK2, PKM2 and LDHA in SAE cells. Cells were infected with hMPV and harvested at different time points of infection to prepare total cell lysates, which were subjected to Western blot analysis to determine levels of expression of HK2, PKM2 and LDHA, key enzymes of the glycolysis pathway. Densitometric analysis of band intensity, normalized to β-actin, is shown to the right.

(Chatham et al., 2008; Wellen et al., 2010).

The first and rate-limiting enzyme in the HBP is glutamine: fructose-6-phosphate aminotransferase 1, GFAT, also called GFPT1. GFPT1 transfers the amide group from glutamine to fructose-6-phosphate to form glucosamine-6-phosphate, a precursor of uridine diphosphate-GlcNAc. The latter is the major substrate for protein N- and O-glycosylation (Wells and Hart, 2003). Our microarray data revealed that GFPT1 mRNA levels were increased by 2.1 fold and 2.4 fold upon hMPV infection at 24 and 48 h respectively. The GFPT2 mRNA levels were also increased by 1.7 and 3.1 fold at 24 and 48 h p.i. respectively, while levels of O-linked N-acetylglucosamine (GlcNAc) transferase (OGT) enzyme were 1.1 and 1.8 fold higher at the same time points (Table 1). To confirm the changes we observed in expression of genes belonging to the hexosamine pathway in A549 cells, SAE cells were infected with hMPV and harvested at various time points p.i. to prepare total RNA or cell lysates. GFPT1 and GFPT2 mRNA levels were analyzed by RT-PCR (Fig. 5**A**), while GFPT1 protein levels were analyzed by Western blot (Fig. 5**B**). There was a time-dependent increase in both GFTP1 and 2 gene expression and GFPT1 protein levels upon hMPV infection, suggesting that this pathway could play an important role in enhancing virus protein glycosylation necessary for production of infectious virus.

2.5. Glycolysis and hexosamine biosynthesis pathway are important for virus replication

To investigate the role of glycolysis on virus replication, we used 2-Deoxy-D-glucose (2DG), a glucose molecule with a 2-hydroxyl group replaced by hydrogen. Inside the cell, 2-DG is converted to phosphorylated 2-DG (2-DG-P) by hexokinase, however, 2-DG-P cannot be metabolized by the second enzyme of the glycolysis pathway, phosphoglucose isomerase. We infected A549 cells with hMPV in presence or absence of 2DG at 5 and 10 uM concentration for 24 h and hMPV titers were measured. We found that compared to untreated cells hMPV titers were decreased in a dose dependent manner at both 5 and 10 uM 2DG concentrations (Fig. 6). We also investigated if inhibition of the glycosylation enzyme OGT, which utilizes substrates provided by the hexosamine pathway, would affect virus replication. A549 cells were infected with hMPV in presence or absence of the OGT inhibitor ST045849 (1 and 5 uM) for 24 h and hMPV titers were determined. We found that OGT inhibition also resulted in significant decreased hMPV production (Fig. 6) compared to untreated cells, strongly suggesting that the enhanced glycolysis and hexosamine pathway, needed for protein glycosylation, play an important role in virus replication.

To further investigate how inhibition of glycolysis affected viral replication, we used several approaches, including quantification of viral gene transcription, genome replication and viral protein detection in cell lysates and cell supernatants. 2DG administration did not significantly decrease the number of RSV genome copies and N gene copies (Fig. 7**A and B**). Expression of the majority of viral proteins, assessed by Western blot assay of total cell lysates, was also not significantly affected by 2DG treatment (Fig. 7**C, anti-hMPV panel**). However, there was a dramatic change in the various form of cellular F protein, in response to 2DG treatment. Specifically the trimeric form of F (F3) was no longer detectable and we could no longer see bands corresponding to F0 and F1 forms, substituted by a single band of a lower molecular weight than the F0 observed in untreated cells. Synthesis of this form of F was also greatly reduced in 2DG treated cells (Fig. 7**C, anti-F panel**). We found that 2DG reduced the presence of high molecular weight G protein and increased the one with lower molecular weight, suggesting a change in the protein glycosylation level (Fig. 7**C, anti-G panel**). To determine whether the reduction in viral titer was due to fewer virus particles released, we performed a western blot analysis of viral proteins in supernatants from cells infected in the absence or presence of 2DG. We found a decrease of viral proteins detected by the anti-hMPV ab (Fig. 7**D, left panel**), and we could not detect F protein in the cell supernatant of treated cells (Fig. 7**D, right panel**), indicating less virus being released in the extracellular space.

3. Discussion

In the past several years, there has been a significant interested in investigating the impact of virus infection on host metabolism, to identify metabolic networks that could be potential targets for development of new antiviral treatments. Metabolomic analysis of infected cells, animal models of virus infection and patients' samples have been performed for HIV, HBV, HCV, Dengue virus, herpesviruses and influenza utilizing methodologies such as GCMS and LCMS [reviewed in (Manchester and Anand, 2017)]. We combined various approaches like microarrays and LCMS/GCMS-based metabolomics to investigate changes induced by hMPV infection in core metabolic pathways of airway epithelial cells. We analyzed more than 5000 genes by IPAs and, not surprisingly, found that approximately 20% of the altered genes in hMPV infected cells were related to metabolism. Interestingly, gene expression of most of the core metabolism enzymes was downregulated in the course of infection, with a few exceptions, such as HK2 of cellular glycolysis and enzymes belonging to the HBP pathway. Protein analysis of normal airway epithelial cells confirmed that HK2, as well as PKM2 and LDHA, were increased upon hMPV infection, which was associated with an increase in some of the upstream glycolysis metabolites, a decrease in pyruvate levels and a significant increase in lactate. These findings, associated with a significant increase of the ADP/ATP ratio, suggest that in the course of hMPV infection glucose is converted to lactate, rather than being metabolized through oxidative phosphorylation in the mitochondria, a far less efficient pathway for ATP generation. In the recent past it has been found that several viruses also induce such changes in core metabolic pathways. Infection with human cytomegalovirus (hCMV), dengue, influenza, adenovirus and the shrimp white spot syndrome virus have been associated with changes in glycolysis, increased lactate production and changes in ATP/ADP ratio

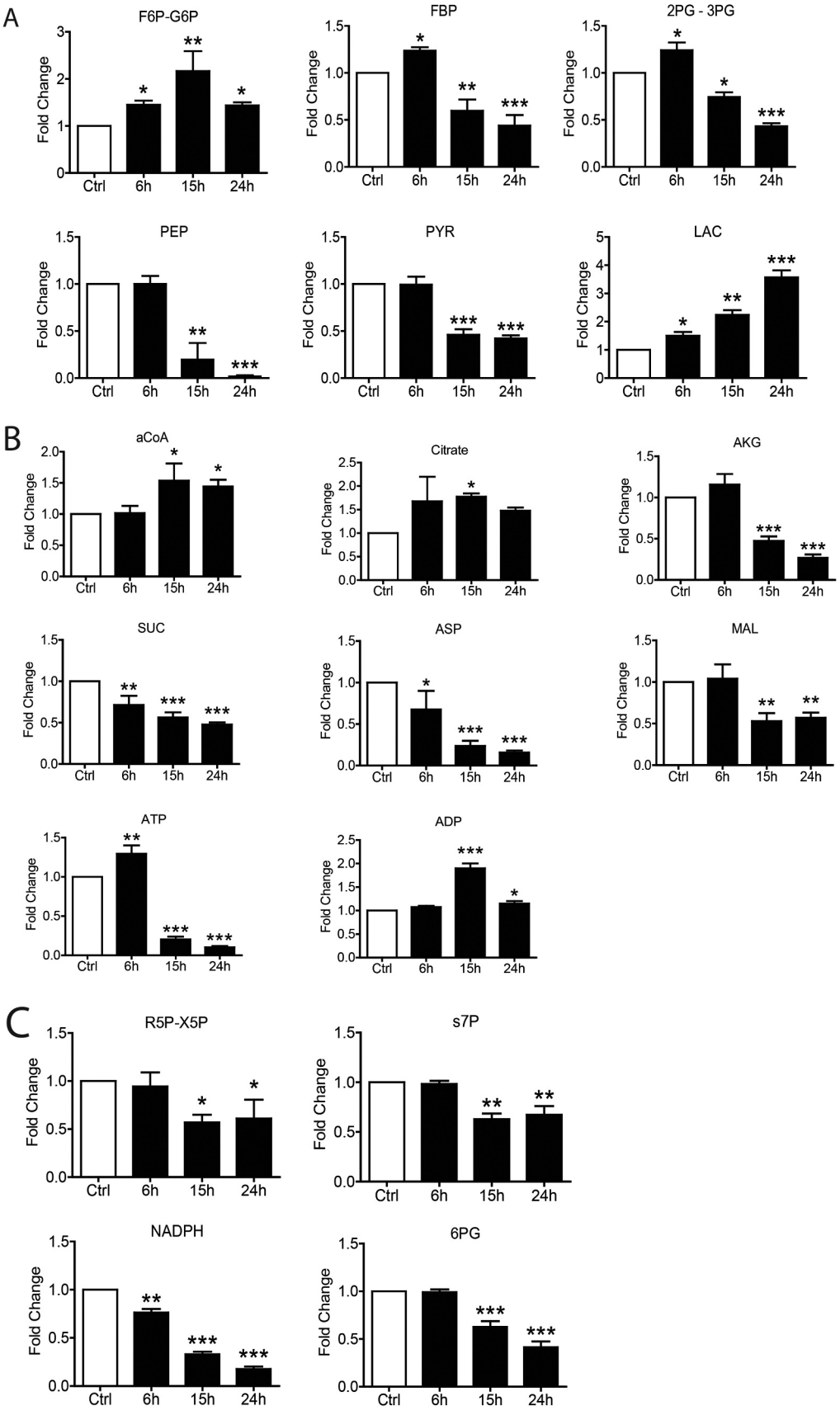

Fig. 4. Metabolomic analysis of Glycolysis/TCA/PPP. SAE cells were infected by hMPV for 0, 6, 15 and 24 h and harvested to measure metabolites belonging to the glycolysis pathway (**A**), TCA pathway (**B**) and pentose phosphate pathway (**C**) by LCMS and GCMS. F6P/G6P- Fructose 6-Phosphate/glucose-6-phosphate, FBP- Fructose 1,6 Biphosphate, 2PG/3PG-2-Phosphoglycerate/3-Phosphoglycerate, PEP- Phosphoenolpyruvate, Pyr- Pyruvate, Lac- Lactate, aCoA- Acetyl-CoA, AKG-Alpha-ketoglutarate, Suc- Succinate, Asp- Aspartate, MAL-Malate, ATP- Adenosine triphosphate, ADP- Adenosine diphosphate, R5P-X5P- D-ribulose-5-phosphate/D-xylulose-5-phosphate, s7P- sedoheptulose-7P, NADPH-Nicotinamide adenine dinucleotide phosphate reduced, 6PG-6-phosphogluconic Acid. Results are expressed as mean ± standard deviation. $^{*}P < 0.05$, $^{**}p < 0.01$, $^{***}p < 0.001$ compared to untreated hMPV-infected cells.

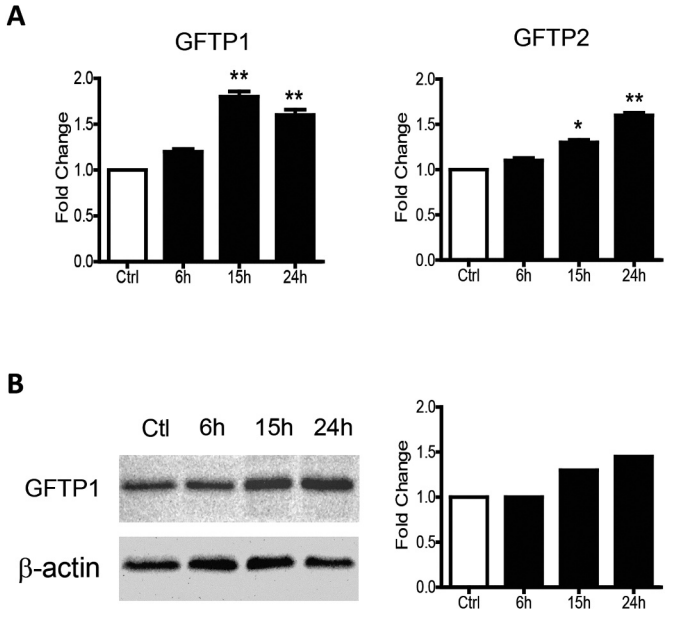

Fig. 5. Expression levels of GFPT1 and 2. SAE cells infected with hMPV were harvested at different time points of infection to (**A**) extract total RNA and assess mRNA levels of GFPT1 and GFPT2 by RT-PCR, or (**B**) prepare total cell lysates and assess GFTP1 by Western blot. Densitometric analysis of band intensity, normalized to β-actin, is shown to the right. Results are expressed as mean ± standard deviation. * $P < 0.05$, ** $p < 0.01$ compared to untreated hMPV-infected cells.

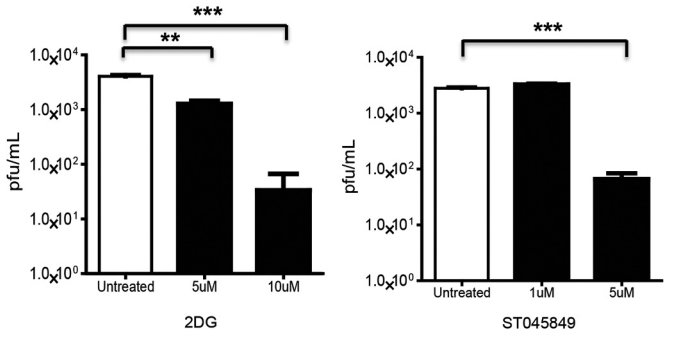

Fig. 6. Effect of inhibition of glycolysis and glycosylation pathway on viral titer. SAE cells were infected with hMPV in the presence or absence of 2DG at 5 and 10 mM or of ST045849 at 1 and 5 mM and harvested at 24 h p.i. to determine viral titer. Results are expressed as mean ± standard deviation. ** $p < 0.01$, *** $p < 0.001$ compared to untreated hMPV-infected cells.

[reviewed in (Sanchez and Lagunoff, 2015; Gonzalez et al., 2016)]. Interference with glycolysis using 2-DG is associated with reduced replication of a variety of viruses, including poliovirus, herpes simplex virus, influenza, respiratory syncytial virus (RSV) and measles [reviewed in (Kang and Hwang, 2006; Sanchez and Lagunoff, 2015)]. A recent study on rhinovirus (RV) infection also found changes in glucose metabolism, with increased uptake and utilization (Gualdoni et al., 2018). Treatment with 2-DG resulted in disruption of RV replication *in vitro* and *in vivo* (Gualdoni et al., 2018).

The TCA cycle plays critical role in both energy production and biosynthesis. Our data show that hMPV infection causes an impairment of the TCA cycle and oxidative phosphorylation resulting in accumulation of acetyl-CoA and citrate. The reduced activity of TCA cycle has been shown to drive citrate into *de novo* synthesis of fatty acid, which has been shown to be necessary for replication of a variety of viruses, including hCMV, dengue and influenza [reviewed in (Sanchez and Lagunoff, 2015)].

Protein glycosylation plays a critical role in overall biochemical complexity in humans. The importance of this protein post-translational modification is emphasized by the fact that about 50% of all proteins are known to be glycosylated and at least 1% of the human genome is represented by glycan biosynthesis genes. The hexosamine biosynthetic pathway (HBP) results in the production of UDP-N-acetylglucosamine (UDP-GlcNAc) and other nucleotide hexosamines. HBP pathway has been associated with viral infection and replication and its involvement with other cell signaling pathways in disease development were recently reported for HCMV and HBV (Li et al., 2015; DeVito et al., 2014). We found that gene expression of key enzymes of the HBP pathways, such as GFPT1 and 2, and the glycosylating enzyme OGT were upregulated in our microarray analysis and we confirmed viral-induced increased expression of GFPT1 and 2 in normal airway epithelial cells. Inhibition of the glycolysis pathway with 2DG and of the glycosylating enzyme OGT with ST045849 dramatically reduced hMPV titers compared to untreated cells, suggesting that both pathways play a crucial role in hMPV replication. Our results indicates that 2DG treatment did not affect viral genome and mRNA production, as well as synthesis of the majority of the viral proteins, but did impact generation of high molecular weight hMPV G protein, which is its highly glycosylated form, and caused a dramatic change in the cellular forms of the F protein, as well as in its synthesis. The trimeric form of F and the bands corresponding to F0 and F1 were no longer detectable after 2DG treatment, while a single band of a molecular weight in between F0 and F1 appeared. Evidence in the literature indicates that F protein glycosylation of hMPV (Zhang et al., 2011) and of other viruses such as Nipah (Moll et al., 2004) is important for F0 processing to F1 + F2, and for surface transport as well, as glycosylated site mutants accumulates in the endoplasmic reticulum, We speculate that the single form of hMPV F protein in 2DG-treated cells could represent an less glycosylated, unprocessed form of F0. Lack of fully functional F and G hampers virion assembly, which could explain the reduction in virus antigen levels in the cell supernatants, likely reflecting less virus particles being present. Reduce/lack of functional F protein in the virion could also account for reduced infectivity of the released virus particles as well.

Overall, our findings further support the evidence of an important relationship between viruses and host cell metabolism, helping the identification of possible therapeutic targets. Both glycolysis and HBP/glycosylation pathways positively regulate hMPV infection (summarized in Fig. 8). It will be important to investigate the manipulation of these pathways in the context of hMPV infection *in vivo*, as 2-DG treatment in a calf model of RSV infection and in a mouse model of RV infection was associated with positive outcomes (Mohanty et al., 1981; Gualdoni et al., 2018), while the same treatment in a mouse model of influenza infection was detrimental (Wang et al., 2016). An in-depth understanding of the cellular mechanisms involved in the metabolism changes triggered by hMPV infection may lead to the discovery of additional novel anti-viral strategies, greatly needed as there is still no effective treatment or vaccine for this important respiratory virus.

4. Materials and methods

4.1. Reagents

Hexokinase 2 (HK2) (cat# 2867), pyruvate kinase M2 (PKM2) (cat# 3198) and lactate dehydrogenase A (LDHA) primary antibodies (cat# 3582) were ordered from Cell Signaling Technology (Beverly, MA, USA). Glutamine-fructose-6-phosphate transaminase 1 (GFPT1) primary antibody was ordered from Abcam (cat# Ab176775, Cambridge, MA, USA). Beta-actin primary antibody (cat# A1978) was ordered from Sigma-Aldrich (St. Louis, MO, USA).). The polyclonal rabbit anti-hMPV whole virus and anti-hMPV G protein antibodies were raised against sucrose-purified hMPVCAN-83. The armenian hamster anti-hMPV F protein antibody was a gift from MedImmune, Mountain View, CA. 2-deoxyglucose (2-DG) was obtained from Sigma-Aldrich and ST045849

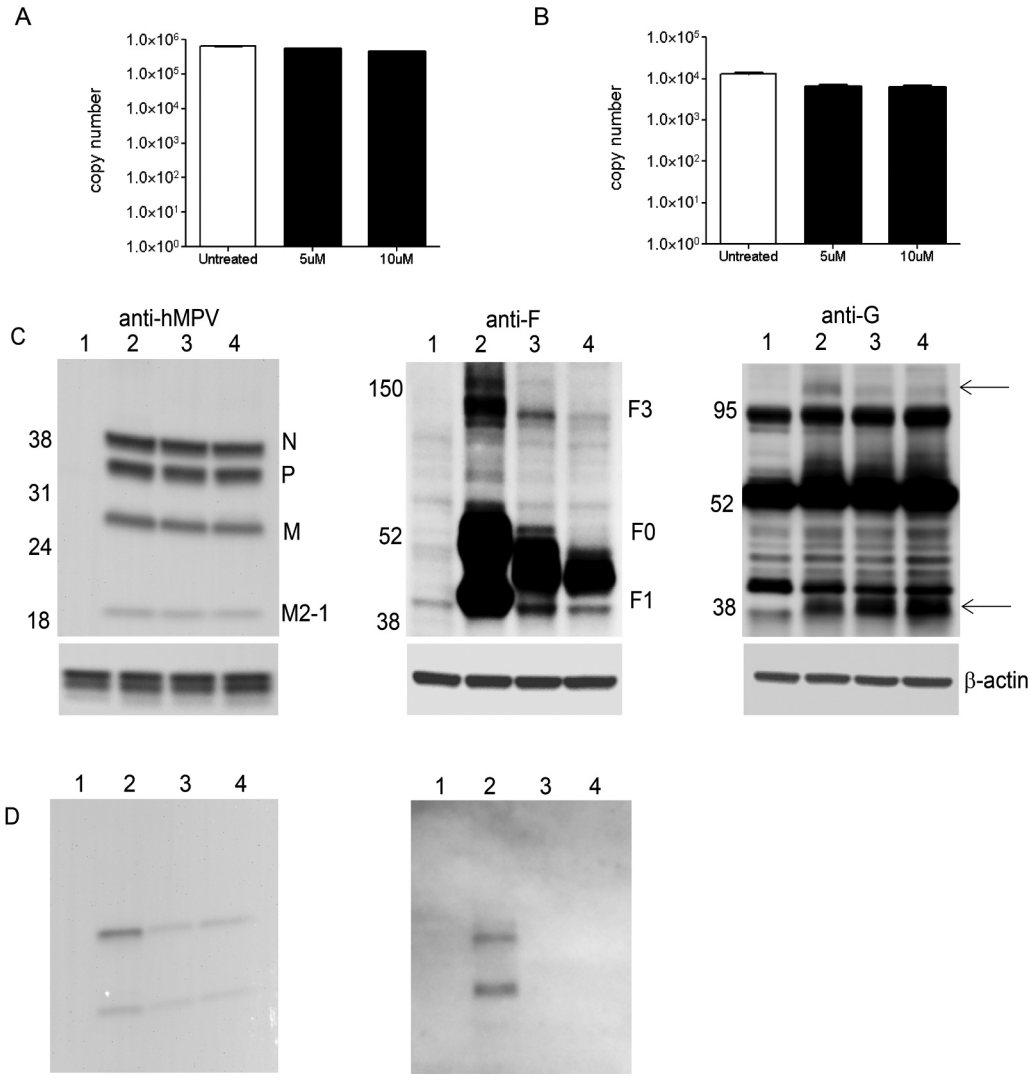

Fig. 7. Effect of 2DG on different steps of viral replication. SAE cells were infected with hMPV in the presence or absence of 2DG at 5 and 10 mM and harvested at 24 h p.i. to prepare either total RNA to measure (**A**) viral genome copies or (**B**) N gene copies by qRT-PCR, or total cell lysates (**C**) to measure viral protein expression by Western blot using an antibody against whole hMPV, anti-F protein or anti-G protein. Membranes were stripped and reprobed with β-actin as a control for equal loading of the samples. Arrows indicate specific bands for the panel using the anti-G protein antibody. (**D**) Cells were infected in the presence or absence of 2DG for 24 h. Cell supernatants were harvested to measure viral protein expression by Western blot using an antibody against whole hMPV or anti-F protein. Lane 1: uninfected; lane 2: infected untreated; lane 3: infected in the presence of 2DG at 5 mM; lane 4: infected in the presence of 2DG at 10 mM.

from TimTec, Newark, DE.

4.2. Cell culture

Human small airway epithelial (SAE) cells (Lonza Walkersville, Inc., MD) were grown in 6-well or 10 cm plates in submerged cultures, according to the manufacturer's instructions, in growth medium containing 0.03 mg/ml bovine pituitary extract (BPE), 0.5 μg/ml hydrocortisone, 0.5 ng/ml hEGF, 0.5 μg/ml epinephrine, 10 μg/ml transferrin, 5 μg/ml insulin, 0.1 ng/ml retinoic acid, 6.5 ng/ml triiodothyronine, 50 μg/ml gentamicin and 50 ng/ml Amphotericin-B, and 0.5 mg/ml bovine serum albumin (BSA, fatty acid free). These cells are guaranteed to be free of mycoplasma contamination. When cells are infected, they are transferred to basal medium, not supplemented with growth factors, 6 h before and throughout the length of the experiment. For all experiments, we used a multiplicity of infection of 3.

4.3. hMPV preparation and virus infection

The hMPV preparation and infection were done as described previously (Bao et al., 2008). In brief, LLC-MK2 cells were infected by virus at a multiplicity of infection (MOI) of 0.01 and the cells were harvested around 5–7 days post-infection. The cells were disrupted and the crude virus was collected and then purified on a sucrose cushion. Viral titer was determined by immunostaining, as previously described (Guerrero-Plata et al., 2006). SAE grown to 80–90% confluence were put into basal medium not supplemented with growth factors for several hours prior to and throughout the infection. Cells were infected with hMPV in serum-free media with 1.0 μg trypsin/ml at a multiplicity of infection (MOI) of 3. Mock-infected cells, defined as control or uninfected cells throughout the manuscript, were treated with same amount of sucrose and the same viral infection media. For 2-DG and ST045849 inhibitor experiments, cells were seeded into 24-well plates, infected with hMPV for 1 h at 37 °C and 5% CO2, and then treated with the specific inhibitor after viral inoculum was removed, throughout the duration of infection. There was no effect of both compounds on uninfected cell viability, assessed by Trypan blue exclusion.

4.4. Western blot

Whole cell lysates were prepared as described previously (Zhao et al., 2011). Briefly, cells were harvested by removing the culture media from the cell plate and washing with ice cold PBS. The cell pellets were harvested in either RIPA buffer or SDS sample buffer containing protease and phosphatase inhibitors. Proteins were fractionated by SDS-PAGE and transferred to polyvinylidene difluoride (PVDF) membranes (Millipore, Bedford, MA). Membranes were blocked in 5% milk for 1 h and then incubated with the indicated primary antibody at 4 °C overnight. Membranes were washed in Tris-buffered saline with 0.1% Tween 20, and incubated with secondary antibody at

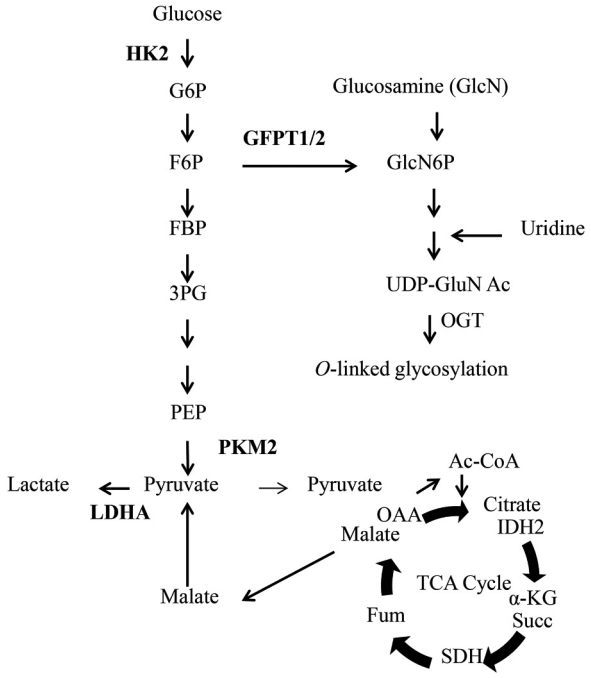

Fig. 8. Core metabolic pathways affected by hMPV infection with key enzymes analyzed in the manuscript highlighted in bold.

room temperature for 1 h. Signals were visualized with an enhanced chemiluminescent (ECL) system onto film. β-actin was used as a loading control. Densitometric analysis of band intensity, normalized to β-actin, was performed using VisionWorks Image Acquisition and Analysis Software (Analytik Jena, Upland, CA).

4.5. Quantitative real-time PCR

Total cellular RNA was extracted using Tri Reagent (Sigma) according to the manufacturer's instructions. A total of 2 μg RNA was used for cDNA preparation by using the SuperScript III First-Strand Synthesis System from Invitrogen (Carlsbad, CA). A total of 1 μL cDNA were amplified in a 10-μL reaction containing 5 μL iQ SYBR Green Supermix (Bio-Rad) and 400 nmol/L primers mixture in 96-well, 0.2-mm thin-wall PCR plates. All reactions were processed in a MyiQ Single Color Real-Time PCR thermocycler (Bio-Rad) using a two-step–plus–melting curve program. For each experimental sample, triplicate reactions were conducted. The ΔΔCt method was used to analyze the experimental data with 18sRNA used as internal standard. Relevant primers were purchased from SA Bioscience (Frederick, MD).

For the absolute N transcript assays, synthetic transcripts of the N gene were generated using the T7 MegaScript kit from Ambion (Austin, TX), treated with Turbo DNase, and purified according to the MegaScript kit protocol. The RT primer to measure the transcription of the hMPV N gene is 5′-CGTCTCAGCCAATCCCTGG**TTTTTTTTTTTTT***AA TTACTC*-3′.

Primers were designed to incorporate a “tag” (underlined letters) as part of the assay due to self-priming exhibited by viral RNA. The tag sequence was derived from the bacterial chloramphenicol resistance (Cm^r) gene. The sequence with bold letters is complementary to poly(A) tails of the transcribed hMPV N gene. The sequence in italic is N gene specific. For the unknown samples, 1 μg of RNA was used. For the synthetic RNA, 10^3 to 10^7 transcripts were used to generate the standard curve. All reactions were performed under the following conditions: 25 °C, 10 min; 48 °C, 30 min; 95 °C, 5 min. Quantitative PCR was performed with 2 μL cDNA and 300 nM N- and tag-specific primers using the FastStart Universal SYBR green master (ROX) (Roche). The hMPV N forward primer was 5′-CACAGACTATTTTCGCAGCAG-3′, and the reverse primer against hMPV tag was 5′-CGTCTCAGCCAATCCC TGG-3′. QPCRs were run in the ABI 7500 sequence detection system under the standard default conditions: initial steps of 50 °C for 2 min and 95 °C for 10 min and PCR steps of 95 °C for 15 s and 60 °C for 1 min, for 40 cycles.

To quantify viral antigenomic copies in the context of hMPV infection, synthetic transcripts of the genome were generated from Topo plasmid containing N-P-M genes, using the T7 MegaScript kit, following the digestion with *Pme*I. The reaction mixture was then treated with Turbo DNase and purified using the MegaScript kit. Primers were designed to span the N and P regions of the viral genome and incorporated a Cm^r tag. First-strand cDNA was transcribed with a P-specific primer, 5′-CGTCTCAGCCAATCCCTGGTGATTATGAGTAATTAAAAAATGGGAC AAG-3′.

The underlined letters indicate the Cm^r tag sequence. QPCRs were performed using the following primers: forward, 5′-CGTCTCAGCCAAT CCCTGG-3′, and reverse, 5′-GCTTCATTACCCATGAAAAGAATATC-3′.

4.6. Microarray data processing and analysis

The detailed information about the data processing and analysis was published in our previous study (Bao et al., 2008). In this study, gene expression data were further analyzed with Benjamini Hochberg method (BH) and for biological function using Ingenuity Pathway Analysis (IPA).

4.7. Metabolomics assays

Cell monolayers were infected with hMPV for the indicated times. After removing the supernatant, cells were rinsed with 150 mM ammonium acetate in water buffer and liquid nitrogen was added directly onto surface of open plates to rapidly freeze cells. Covered plates were transferred to cooler with dry ice and stored at -800C until ready for extraction and metabolomics analysis by gas chromatography-mass spectrometry (GC/MS) and liquid chromatography-mass spectrometry (LC/MS). Assays were performed by the University of Michigan Metabolomics Core.

4.8. Statistical analysis

Unpaired parametrical (*t*-test) or non-parametrical (Mann-Whitney) tests were used to compare two groups at a time. One-way analysis of variance (ANOVA) with Tukey's post-hoc analysis was used in multiple comparisons. Null hypotheses were rejected at *P* values less than 0.05. All data are presented in figures represent means ± standard deviation (* $p < 0.05$, ** $p < 0.01$, *** $p < 0.001$). Experiments were performed a minimum of three times. Statistical analysis was performed with GraphPad Prism 5 software (GraphPad Software, Inc., La Jolla, CA).

Acknowledgements

We thank late Mala Sinha for her help with microarray data analysis. We also thank Tianshuang Liu for her technical support, and Cynthia Tribble for her help with manuscript editing and submission.

Funding

This work was partially supported by National Institutes of Health grants AI0799246 and AI062885 and it utilized Core Services supported by grant DK097153 to the University of Michigan.

Appendix A. Supporting information

Supplementary data associated with this article can be found in the online version at doi:10.1016/j.virol.2019.03.011.

References

Afonso, C.L., Amarasinghe, G.K., Banyai, K., Bao, Y., Basler, C.F., Bavari, S., Bejerman, N., Blasdell, K.R., Briand, F.X., Briese, T., Bukreyev, A., Calisher, C.H., Chandran, K., Cheng, J., Clawson, A.N., Collins, P.L., Dietzgen, R.G., Dolnik, O., Domier, L.L., Durrwald, R., Dye, J.M., Easton, A.J., Ebihara, H., Farkas, S.L., Freitas-Astua, J., Formenty, P., Fouchier, R.A., Fu, Y., Ghedin, E., Goodin, M.M., Hewson, R., Horie, M., Hyndman, T.H., Jiang, D., Kitajima, E.W., Kobinger, G.P., Kondo, H., Kurath, G., Lamb, R.A., Lenardon, S., Leroy, E.M., Li, C.X., Lin, X.D., Liu, L., Longdon, B., Marton, S., Maisner, A., Muhlberger, E., Netesov, S.V., Nowotny, N., Patterson, J.L., Payne, S.L., Paweska, J.T., Randall, R.E., Rima, B.K., Rota, P., Rubbenstroth, D., Schwemmle, M., Shi, M., Smither, S.J., Stenglein, M.D., Stone, D.M., Takada, A., Terregino, C., Tesh, R.B., Tian, J.H., Tomonaga, K., Tordo, N., Towner, J.S., Vasilakis, N., Verbeek, M., Volchkov, V.E., Wahl-Jensen, V., Walsh, J.A., Walker, P.J., Wang, D., Wang, L.F., Wetzel, T., Whitfield, A.E., Xie, J.T., Yuen, K.Y., Zhang, Y.Z., Kuhn, J.H., 2016. Taxonomy of the order Mononegavirales: update 2016. Arch. Virol. 161, 2351–2360.

Bao, X., Sinha, M., Liu, T., Hong, C., Luxon, B.A., Garofalo, R.P., Casola, A., 2008. Identification of human metapneumovirus-induced gene networks in airway epithelial cells by microarray analysis. Virol. (New Y. NY) 374, 114–127.

Biacchesi, S., Pham, Q.N., Skiadopoulos, M.H., Murphy, B.R., Collins, P.L., Buchholz, U.J., 2006. Modification of the trypsin-dependent cleavage activation site of the human metapneumovirus fusion protein to be trypsin independent does not increase replication or spread in rodents or nonhuman primates. J. Virol. 80, 5798–5806.

Chambers, J.W., Maguire, T.G., Alwine, J.C., 2010. Glutamine metabolism is essential for human cytomegalovirus infection. J. Virol. 84, 1867–1873.

Chatham, J.C., Not, L.G., Fulop, N., Marchase, R.B., 2008. Hexosamine biosynthesis and protein O-glycosylation: the first line of defense against stress, ischemia, and trauma 15. Shock 29, 431–440.

DeVito, S.R., Ortiz-Riano, E., Martinez-Sobrido, L., Munger, J., 2014. Cytomegalovirus-mediated activation of pyrimidine biosynthesis drives UDP-sugar synthesis to support viral protein glycosylation. Proc. Natl. Acad. Sci. USA 111, 18019–18024.

Gonzalez Plaza, J.J., Hulak, N., Kausova, G., Zhumadilov, Z., Akilzhanova, A., 2016. Role of metabolism during viral infections, and crosstalk with the innate immune system. Intractable Rare. Dis. Res. 5, 90–96.

Gualdoni, G.A., Mayer, K.A., Kapsch, A.M., Kreuzberg, K., Puck, A., Kienzl, P., Oberndorfer, F., Fruhwirth, K., Winkler, S., Blaas, D., Zlabinger, G.J., Stockl, J., 2018. Rhinovirus induces an anabolic reprogramming in host cell metabolism essential for viral replication. Proc. Natl. Acad. Sci. USA 115, E7158–E7165.

Guerrero-Plata, A., Casola, A., Suarez, G., Yu, X., Spetch, L., Peeples, M.E., Garofalo, R.P., 2006. Differential response of dendritic cells to human metapneumovirus and respiratory syncytial virus. Am. J. Respir. Cell Mol. Biol. 34, 320–329.

Kahn, J.S., 2006. Epidemiology of human metapneumovirus. Clin. Microbiol. Rev. 19, 546–557.

Kang, H.T., Hwang, E.S., 2006. 2-Deoxyglucose: an anticancer and antiviral therapeutic, but not any more a low glucose mimetic. Life Sci. (Oxf.) 78, 1392–1399.

Li, H.D., Zhu, W.D., Zhang, L.K., Lei, H.H., Wu, X.Y., Guo, L., Chen, X.W., Wang, Y.L., Tang, H.R., 2015. The metabolic responses to hepatitis B virus infection shed new light on pathogenesis and targets for treatment. Sci. Rep. 5, 8421.

Manchester, M., Anand, A., 2017. Metabolomics: strategies to define the role of metabolism in virus infection and pathogenesis. Adv. Virus Res. 98, 57–81.

Mohanty, S.B., Rockemann, D.D., Davidson, J.P., Tripathy, R.N., Ingling, A.L., 1981. Chemotherapeutic effect of 2-deoxy-D-glucose against respiratory syncytial viral infection in calves. Am. J. Vet. Res. 42, 336–338.

Moll, M., Kaufmann, A., Maisner, A., 2004. Influence of N-glycans on processing and biological activity of the nipah virus fusion protein. J. Virol. 78, 7274–7278.

Munger, J., Bajad, S.U., Coller, H.A., Shenk, T., Rabinowitz, J.D., 2006. Dynamics of the cellular metabolome during human cytomegalovirus infection. PLoS Pathog. 2, 1165–1175.

Munger, J., Bennett, B.D., Parikh, A., Feng, X.J., McArdle, J., Rabitz, H.A., Shenk, T., Rabinowitz, J.D., 2008. Systems-level metabolic flux profiling identifies fatty acid synthesis as a target for antiviral therapy. Nat. Biotechnol. 26, 1179–1186.

Sanchez, E.L., Lagunoff, M., 2015. Viral activation of cellular metabolism 1. Virology (New Y. NY) 479, 609–618.

Vander Heiden, M.G., Cantley, L.C., Thompson, C.B., 2009. Understanding the Warburg effect: the metabolic requirements of cell proliferation 2. Science (Wash. DC) 324, 1029–1033.

Wang, A., Huen, S.C., Luan, H.H., Yu, S., Zhang, C., Gallezot, J.D., Booth, C.J., Medzhitov, R., 2016. Opposing Effects of Fasting Metabolism on Tissue Tolerance in Bacterial and Viral Inflammation. Cell (Camb. MA) 166, 1512–1525.

Wellen, K.E., Lu, C., Mancuso, A., Lemons, J.M.S., Ryczko, M., Dennis, J.W., Rabinowitz, J.D., Coller, H.A., Thompson, C.B., 2010. The hexosamine biosynthetic pathway couples growth factor-induced glutamine uptake to glucose metabolism 2. Genes Dev. 24, 2784–2799.

Wells, L., Hart, G.W., 2003. O-GlcNAc turns twenty: functional implications for post-translational modification of nuclear and cytosolic proteins with a sugar 2. FEBS Lett. 546, 154–158.

Zhang, J., Dou, Y., Wu, J., She, W., Luo, L., Zhao, Y., Liu, P., Zhao, X., 2011. Effects of N-linked glycosylation of the fusion protein on replication of human metapneumovirus in vitro and in mouse lungs. J. General. Virol. 92, 1666–1675.

Zhao, Y., Banerjee, S., LeJeune, W.S., Choudhary, S., Tilton, R.G., 2011. NF-kappaB-inducing kinase increases renal tubule epithelial inflammation associated with diabetes 15. Exp. Diabetes Res. 2011, 192564.